Prepared for submission to JHEP

Measurements of K_S^0-K_L^0 asymmetries in the decays $\Lambda_c^+ \to pK_{L,S}^0$, $pK_{L,S}^0\pi^+\pi^-$ and $pK_{L,S}^0\pi^0$

The BESIII collaboration

E-mail: besiii-publications@ihep.ac.cn

Abstract: Using e^+e^- annihilation data sets corresponding to an integrated luminosity of 4.5 fb^{-1}, collected with the BESIII detector at center-of-mass energies between 4.600 and 4.699 GeV, we report the first measurements of the absolute branching fractions $\mathcal{B}(\Lambda_c^+ \to pK_L^0) = (1.67 \pm 0.06 \pm 0.04)\%$, $\mathcal{B}(\Lambda_c^+ \to pK_L^0\pi^+\pi^-) = (1.69 \pm 0.10 \pm 0.05)\%$, and $\mathcal{B}(\Lambda_c^+ \to pK_L^0\pi^0) = (2.02 \pm 0.13 \pm 0.05)\%$, where the first uncertainties are statistical and the second systematic. Combining with the known branching fractions of $\Lambda_c^+ \to pK_S^0$, $\Lambda_c^+ \to pK_S^0\pi^+\pi^-$, and $\Lambda_c^+ \to pK_S^0\pi^0$, we present the first measurements of the K_S^0-K_L^0 asymmetries $R(\Lambda_c^+, K_{S,L}^0X) = \frac{\mathcal{B}(\Lambda_c^+\to K_S^0X)-\mathcal{B}(\Lambda_c^+\to K_L^0X)}{\mathcal{B}(\Lambda_c^+\to K_S^0X)+\mathcal{B}(\Lambda_c^+\to K_L^0X)}$ in charmed baryon decays: $R(\Lambda_c^+, pK_{S,L}^0) = -0.025 \pm 0.031$, $R(\Lambda_c^+, pK_{S,L}^0\pi^+\pi^-) = -0.027 \pm 0.048$, and $R(\Lambda_c^+, pK_{S,L}^0\pi^0) = -0.015 \pm 0.046$. No significant asymmetries within the uncertainties are observed.

Keywords: Λ_c^+ baryon, K_S^0-K_L^0 asymmetry, the BESIII detector

ArXiv ePrint: 1234.56789

Contents

1 Introduction

The lightest charmed baryon, Λ_c^+, provides a unique environment for studying the behavior of light di-quarks in the presence of a heavy quark [1]. Its hadronic decays occur only through the weak interaction, and various theoretical models have been proposed. These include the covariant confined quark model [2, 3], the pole model [4–9], current algebra [10, 11], and SU(3) flavor symmetry approaches [12–16]. Its decay falls into three categories: Cabibbo-favored (CF) decays, singly Cabibbo-suppressed decays, and doubly Cabibbo-suppressed (DCS) decays. The decay amplitudes of the CF and DCS modes are expected to be proportional to the products of the Cabibbo-Kobayashi-Maskawa elements $|V_{ud}^*V_{cs}|$ and $|V_{us}^*V_{cd}|$, respectively. The ratio of their decays is approximately of the order of $\mathcal{O}(10^{-3})$, resulting in a small branching fraction (BF) for the DCS decay and making it challenging to observe directly in experiments.

In addition to direct measurements of DCS decays, the amplitudes of DCS modes can be probed using the K_S^0-K_L^0 asymmetry in the decays into neutral kaons, which arises from the interference between CF and DCS amplitudes [17, 18]. The K_S^0-K_L^0 asymmetry has been studied in the decays of charmed D mesons, where the asymmetry is defined by

$$R(D, K_{S,L}^0X) = \frac{\mathcal{B}(D \to K_S^0X) - \mathcal{B}(D \to K_L^0X)}{\mathcal{B}(D \to K_S^0X) + \mathcal{B}(D \to K_L^0X)}, \tag{1.1}$$

and X can be π^0, η, η', ω, ρ^0 or ϕ. A large asymmetry for $R(D^0, K_{S,L}^0\pi^0)$ was reported in a previous measurement by the CLEO experiment as $R(D^0, K_{S,L}^0\pi^0) = 0.108 \pm 0.025 \pm 0.024$ [19], where the first uncertainty is statistical and the second is systematic. The BESIII experiment reported measurements of the K_S^0-K_L^0 asymmetries $R(D^0, K_{S,L}^0X)$, where $X = \phi$, η, ω [20]. Significant asymmetries were observed in $D^0 \to K_L^0\eta$ and $D^0 \to K_L^0\eta'$

decays with $R(D^0, K^0_{S,L}\eta) = 0.080 \pm 0.022$ and $R(D^0, K^0_{S,L}\eta') = 0.108 \pm 0.035$, respectively. In addition, this asymmetry has been investigated for the lightest charmed strange meson, and $R(D_s^+, K^0_{S,L}K^+)$ was determined to be $(-2.1 \pm 1.9 \pm 1.6)\%$ [21]. However, such measurements have not been made for the decays of charmed baryons.

Using flavor SU(3) asymmetry [12–16], theoretical predictions [18] for K^0_S-K^0_L asymmetries have been made for charmed baryon two-body decays into a light baryon and a neutral kaon. Similar to Equation 1.1, the asymmetry of $\mathcal{B}(\Lambda_c^+ \to K^0_S X)$ and $\mathcal{B}(\Lambda_c^+ \to K^0_L X)$ in charmed baryon decays is defined as

$$R(\Lambda_c^+, K^0_{S,L}X) = \frac{\mathcal{B}(\Lambda_c^+ \to K^0_S X) - \mathcal{B}(\Lambda_c^+ \to K^0_L X)}{\mathcal{B}(\Lambda_c^+ \to K^0_S X) + \mathcal{B}(\Lambda_c^+ \to K^0_L X)}, \tag{1.2}$$

where X is p, $p\pi^+\pi^-$ or $p\pi^0$. Equation 1.2 can be further reduced as $R(\Lambda_c^+ \to K^0_{S,L}X) \simeq -2r_f \cos\delta_f$, where r_f and δ_f are the relative strength and phase between the DCS ($\Lambda_c^+ \to K^0 X$) and CF ($\Lambda_c^+ \to \bar{K}^0 X$) amplitudes, respectively. The parameter r_f is expected to be proportional to the ratio $|V^*_{cd}V_{us}/V^*_{cs}V_{ud}| \sim \lambda^2$ [22]. A non-zero asymmetry value indicates the presence of DCS processes. The asymmetry of $\Lambda_c^+ \to pK^0_{S,L}$ is predicted to be in the range of (−0.010, 0.087) in Ref. [18]. The K^0_S-K^0_L asymmetry is a promising observable with which to search for the two-body DCS processes of charmed baryons.

In this paper, we report the first measurements of the absolute BFs of $\Lambda_c^+ \to pK^0_L$, $\Lambda_c^+ \to pK^0_L\pi^+\pi^-$ and $\Lambda_c^+ \to pK^0_L\pi^0$ based on e^+e^- annihilation data samples corresponding to a total integrated luminosity of 4.5 fb^{-1} collected at the center-of-mass (c.m.) energies $\sqrt{s}$ between 4.600 and 4.699 GeV. The luminosities are listed in Table 1 [23, 24]. Using the results of $\mathcal{B}(\Lambda_c^+ \to pK^0_S)$, $\mathcal{B}(\Lambda_c^+ \to pK^0_S\pi^+\pi^-)$, and $\mathcal{B}(\Lambda_c^+ \to pK^0_S\pi^0)$ from the Particle Data Group (PDG) [22], we present the K^0_S-K^0_L asymmetries $R(\Lambda_c^+, K^0_{S,L}X)$, where $X = p$, $p\pi^+\pi^-$ or $p\pi^0$. Charge conjugate channels are implied throughout this paper, unless explicitly stated.

Table 1. The integrated luminosities at each c.m. energy [23, 24].

$\sqrt{s}$ (GeV)	Integrated luminosity (pb^{-1})
4.600	586.9 ± 0.1 ± 3.9
4.612	103.7 ± 0.1 ± 0.6
4.628	521.5 ± 0.1 ± 2.8
4.641	551.7 ± 0.1 ± 2.9
4.661	529.4 ± 0.1 ± 2.8
4.682	1667.4 ± 0.2 ± 8.8
4.699	535.5 ± 0.1 ± 2.8

2 BESIII experiment and Monte Carlo simulation

The BESIII detector [25] records symmetric e^+e^- collisions provided by the BEPCII storage ring [26], which operates at c.m. energies ranging from 1.85 to 4.95 GeV, with a peak luminosity of 1.1×10^{33} cm^{-2}s^{-1} achieved at $\sqrt{s} = 3.773$ GeV. The BESIII detector has collected large data samples in this energy region [27]. The cylindrical core of the BESIII detector covers 93% of the full solid angle and consists of a helium-based multilayer drift chamber (MDC), a plastic scintillator time-of-flight system (TOF), and a CsI(Tl) electromagnetic calorimeter (EMC), which are all enclosed in a superconducting solenoidal magnet providing a 1.0 T magnetic field [28]. The solenoid is supported by an octagonal flux-return yoke with resistive plate counter muon identification modules interleaved with steel. The charged-particle momentum resolution at $1\,\mathrm{GeV}/c$ is 0.5%, and the $\mathrm{d}E/\mathrm{d}x$ resolution is 6% for electrons from Bhabha scattering. The EMC measures photon energies with a resolution of 2.5% (5%) at 1 GeV in the barrel (end cap) region. The time resolution in the TOF barrel region is 68 ps, while that in the end cap region was initially 110 ps. The end cap TOF system was upgraded in 2015 using multi-gap resistive plate chamber technology, providing a time resolution of 60 ps [29–31]. Of the data used in this analysis, 87% was with the upgraded end cap TOF.

Simulated samples generated with GEANT4-based [32] Monte Carlo (MC) software, which includes the geometric description of the BESIII detector and the detector response performance [28, 33, 34], are used to determine detection efficiencies and to estimate potential background contributions. The simulation describes the beam energy spread and the initial state radiation (ISR) in the e^+e^- annihilations with the generator KKMC [35, 36]. The inclusive MC samples, corresponding to about 40 times the number of events of the data samples, include the production of $\Lambda_c^+\bar{\Lambda}_c^-$ pairs, open charm processes, the ISR production of vector charmonium(-like) states, and the continuum processes incorporated in KKMC [35, 36]. The known decay modes are modeled with EVTGEN [31, 37] using BFs taken from the PDG [22], and the remaining unknown charmonium decays are modeled with LUNDCHARM [31, 38]. Final state radiation from charged final state particles is incorporated using PHOTOS [39]. For the production of $e^+e^- \to \Lambda_c^+\bar{\Lambda}_c^-$ events, the Born cross-section line shape from BESIII measurements is used [40, 41]. Exclusive $e^+e^- \to \Lambda_c^+\bar{\Lambda}_c^-$ signal MC samples are generated with $\bar{\Lambda}_c^-$ decaying to twelve specific tag modes (as described in Section 3) and Λ_c^+ decaying to pK_L^0, $pK_L^0\pi^+\pi^-$ and $pK_L^0\pi^0$. The angular distribution of the decay $\Lambda_c^+ \to pK_L^0$ is modeled with decay asymmetry parameters obtained from Ref. [42]. For processes from $\Lambda_c^+ \to pK_L^0\pi^+\pi^-$ and $\Lambda_c^+ \to pK_L^0\pi^0$ channels, signal models are tunned based on the data. Additional MC samples are generated to estimate contributions from peaking background processes, where $\bar{\Lambda}_c^-$ decays into tag modes and Λ_c^+ decays into pK_S^0, $p\eta$, $pK_S^0\pi^0$, and $pK_S^0\pi^+\pi^-$, with K_S^0 and η decaying inclusively. Each tag mode of the exclusive MC samples is generated with the same number of events.

3 Data analysis

Taking advantage of the threshold production of the $\Lambda_c^+\bar{\Lambda}_c^-$ pair, the double-tag (DT) method [43–46] is employed to study $\Lambda_c^+ \to pK_L^0$, $\Lambda_c^+ \to pK_L^0\pi^+\pi^-$ and $\Lambda_c^+ \to pK_L^0\pi^0$, where K_L^0 is reconstructed by the missing-mass technique. A single-tag (ST) event is selected by tagging a $\bar{\Lambda}_c^-$ baryon with one of the following twelve tag modes: $\bar{p}K_S^0$, $\bar{p}K^+\pi^-$, $\bar{p}K_S^0\pi^0$, $\bar{p}K_S^0\pi^-\pi^+$, $\bar{p}K^+\pi^-\pi^0$, $\bar{p}\pi^-\pi^+$, $\bar{\Lambda}\pi^-$, $\bar{\Lambda}\pi^-\pi^0$, $\bar{\Lambda}\pi^-\pi^+\pi^-$, $\bar{\Sigma}^0\pi^-$, $\bar{\Sigma}^-\pi^0$, and $\bar{\Sigma}^-\pi^-\pi^+$.

The ST event selection criteria, efficiencies, and yields are described in Ref. [47]. The signal decays $\Lambda_c^+ \to pK_L^0$, $pK_L^0\pi^+\pi^-$, and $pK_L^0\pi^0$ are reconstructed using the remaining charged tracks and photons recoiling against the ST $\bar{\Lambda}_c^-$ candidates, and referred to as DT events.

Charged tracks are required to be within $|\cos\theta| < 0.93$, where θ is the polar angle defined with respect to the z-axis, which is the symmetry axis of the MDC. The distance of closest approach to the interaction point (IP) must be less than 10 cm along the z axis and less than 1 cm in the perpendicular plane. Particle identification (PID) for charged tracks combines measurements of the energy deposited in the MDC (dE/dx) and the flight time in the TOF to form a likelihood value $\mathcal{L}(h)$ for each hadron (h) hypothesis, where $h = p, K$, or π. Charged tracks are identified as protons if the proton hypothesis has the highest likelihood ($\mathcal{L}(p) > \mathcal{L}(K)$ and $\mathcal{L}(p) > \mathcal{L}(\pi)$), or as pions if $\mathcal{L}(\pi) > \mathcal{L}(K)$ is satisfied.

Photon candidates are reconstructed from showers that are not associated with any charged tracks in the EMC [25]. The deposited energy of each shower in the EMC is required to be greater than 25 MeV in the barrel region ($|\cos\theta| < 0.80$), and greater than 50 MeV in the end cap region ($0.86 < |\cos\theta| < 0.92$). The EMC time difference from the event start time is required to be less than 700 ns, to exclude electronic noise and showers unrelated to the events. The opening angle between each shower and $\bar{p}$ must be greater than 20°, to suppress the background from annihilation of $\bar{p}$ with the detector material. The π^0 candidates are reconstructed from photon pairs with invariant mass $M(\gamma\gamma)$ in the range 0.115 GeV$/c^2 < M(\gamma\gamma) < 0.150$ GeV$/c^2$. To improve momentum resolution and exclude background, a kinematic fit is performed to constrain $M(\gamma\gamma)$ to the known π^0 mass [22], and candidates with fit quality $\chi^2 < 20$ are retained for further analysis.

The signal candidates of $\Lambda_c^+ \to pK_L^0$ and $\Lambda_c^+ \to pK_L^0\pi^0$ are required to have only one charged track with opposite charge to the tagged $\bar{\Lambda}_c^-$ satisfying the proton PID criteria. For $\Lambda_c^+ \to pK_L^0\pi^0$ decay, the π^0 candidate with the highest energy is selected. In the reconstruction of $\Lambda_c^+ \to pK_L^0\pi^+\pi^-$, events must have only three remaining charged tracks with correct charges and PID. Candidates with additional charged tracks, whose distances of closest approaches to the IP are within ± 20 cm along the beam direction, are excluded. The presence of the K_L^0 is inferred by the kinematic variable $M^2_{\rm miss}$, defined as

$$M^2_{\rm miss} \equiv \left(E_{\rm beam} - E_{\rm selected}\right)^2/c^4 - \left|\vec{p}_{\Lambda_c^+} - \vec{p}_{\rm selected}\right|^2/c^2, \tag{3.1}$$

where $E_{\rm beam}$ is the beam energy and $E_{\rm selected}$ ($\vec{p}_{\rm selected}$) is the total measured energy (momentum) of the selected particles in the DT signal side, boosted into the c.m. system of e^+e^-. To improve the momentum resolution, the momentum of Λ_c^+ is determined by

$$\vec{p}_{\Lambda_c^+} \equiv -\hat{p}_{\bar{\Lambda}_c^-}\sqrt{E^2_{\rm beam}/c^2 - m^2_{\Lambda_c^+}c^2}, \tag{3.2}$$

where $\hat{p}_{\bar{\Lambda}_c^-}$ is the direction of the tagged $\bar{\Lambda}_c^-$ and $m_{\Lambda_c^+}$ is the known Λ_c^+ baryon mass taken from the PDG [22]. For all three decays, the $M^2_{\rm miss}$ distributions are expected to have a peak around the known mass squared of K_L^0 [22].

Based on studies of inclusive MC samples, the dominant background events for the signal mode $\Lambda_c^+ \to pK_L^0\pi^+\pi^-$ are from processes with $\Lambda \to p\pi^-$ and $K_S^0 \to \pi^+\pi^-$. They are rejected by vetoing events with $M(p\pi^-)$ ($M(\pi^+\pi^-)$) invariant masses in the interval of 1.11 GeV/c^2 < $M(p\pi^-)$ < 1.12 GeV/c^2 (0.48 GeV/c^2< $M(\pi^+\pi^-)$ < 0.52 GeV/c^2). The combinatorial backgrounds are suppressed by requiring the recoil mass of the proton $M_{\rm recoil}(p) \equiv \sqrt{E_{\rm beam}^2 - |\vec{p}_{\Lambda_c^+} - \vec{p}_p|^2} > 1.0$ GeV/c^2, which removes only about 3% of the signal. Here $\vec{p}_p$ is the momentum of the proton. For the $\Lambda_c^+ \to pK_L^0\pi^0$ signal mode, background events of $\Lambda_c^+ \to pK_S^0(\to \pi^0\pi^0)$ and pK_L^0 are excluded by requiring $M_{\rm recoil}(p) >$ 0.65GeV/c^2, which removes less than 1% of signal. Events within the range 1.17 GeV/c^2 < $M(p\pi^0)$ < 1.20 GeV/c^2 are discarded to suppress the background of the $\Sigma^+ \to p\pi^0$ decay.

To improve the momentum resolution, a six constraint (6C) kinematic fit is performed requiring total four-momentum conservation with respect to that of the initial e^+e^- collision and constraining both masses of the tagged $\bar{\Lambda}_c^-$ and the signal Λ_c^+ to $m_{\Lambda_c^+}$. The K_L^0 is treated as a missing particle, and its four-momentum and mass are free in the kinematic fit. The χ^2 of the kinematic fit for each signal mode is required to be less than the optimized value that maximizes the figure of merit $S/\sqrt{S+B}$, where S and B are the numbers of signal and background events from MC simulations, scaled to the data luminosity. The optimized requirements are $\chi^2 < 60$ for $\Lambda_c^+ \to pK_L^0$, $\chi^2 < 25$ for $\Lambda_c^+ \to pK_L^0\pi^+\pi^-$, and $\chi^2 < 20$ for $\Lambda_c^+ \to pK_L^0\pi^0$. The resulting $M_{\rm miss}^2$ distributions of the DT events are shown in Figure 1, which combine all data samples at the seven c.m. energies. Signal events are indicated by the significant peaks around the K_L^0 mass squared.

There are peaking backgrounds remaining from $\Lambda_c^+ \to pK_S^0(\to \pi^0\pi^0)$ and $\Lambda_c^+ \to p\eta(\to \gamma\gamma$ or $3\pi^0)$, $\Lambda_c^+ \to pK_S^0(\to \pi^0\pi^0)\pi^+\pi^-$, and $\Lambda_c^+ \to pK_S^0(\to \pi^0\pi^0)\pi^0$ in the corresponding signal modes. The peaking background events from $\Lambda_c^+ \to K_S^0X$ decays $N_{K_S^0X}^{\rm Bkg}$ are determined by

$$N_{K_S^0X}^{\rm Bkg} = N_{{\rm DT}\,K_S^0X}^{\rm Data} \cdot w_{K_S^0X},\ w_{K_S^0X} = \frac{\sum_i s_i \cdot \frac{N_i^{\rm ST}}{\varepsilon_i^{\rm ST}} \cdot N_{{\rm DT}\,K_L^0X}^{{\rm MC},i}}{\sum_i \frac{N_i^{\rm ST}}{\varepsilon_i^{\rm ST}} \cdot N_{{\rm DT}\,K_S^0X}^{{\rm MC},i}}, \tag{3.3}$$

where i represents the tag mode, and $N_{{\rm DT}\,K_S^0X}^{\rm Data}$ denotes the data yields passing the DT selection criteria of $\Lambda_c^+ \to K_S^0X$. Here, the DT selection criteria of $\Lambda_c^+ \to K_S^0X$ require a fully reconstructed K_S^0 from $\pi^+\pi^-$ combinations, as described in Ref. [48]. $N_{{\rm DT}\,K_S^0X}^{\rm Data}$ is corrected by the factor $w_{K_S^0X}$, which is derived from the exclusive MC simulation samples of $\Lambda_c^+ \to K_S^0X$. $N_{{\rm DT}\,K_L^0X}^{{\rm MC},i}$ and $N_{{\rm DT}\,K_S^0X}^{{\rm MC},i}$ are the numbers of the K_S^0X MC events that satisfy the DT selection criteria of $\Lambda_c^+ \to K_L^0X$ and $\Lambda_c^+ \to K_S^0X$, respectively. $N_i^{\rm ST}$ and $\varepsilon_i^{\rm ST}$ are the ST yields and ST efficiencies from Ref. [47]. A scale factor s_i is specified for each tag mode, and s_i is set to 2 if both the tag and signal modes are K_S^0X. Otherwise, it is set to 1. For peaking background events from $\Lambda_c^+ \to p\eta$, the contribution is evaluated based on the corresponding exclusive MC samples using

$$N_{p\eta}^{\rm Bkg} = \mathcal{B}(\Lambda_c^+ \to p\eta) \cdot w_{p\eta},\ w_{p\eta} = \sum_i \left(\frac{N_i^{\rm ST}}{\varepsilon_i^{\rm ST}} \cdot \frac{N_{pK_L^0}^{\prime{\rm MC},i}}{N_{\rm tot}^{\prime{\rm MC},i}} \right), \tag{3.4}$$

with $\mathcal{B}(\Lambda_c^+ \to p\eta) = (1.41 \pm 0.11) \times 10^{-3}$ [22]. $N_{pK_L^0}^{\prime{\rm MC},i}$ is the number of surviving DT events for the i-th tag mode, that satisfy the DT selection criteria of $\Lambda_c^+ \to pK_L^0$, and $N_{\rm tot}^{\prime{\rm MC},i}$ is

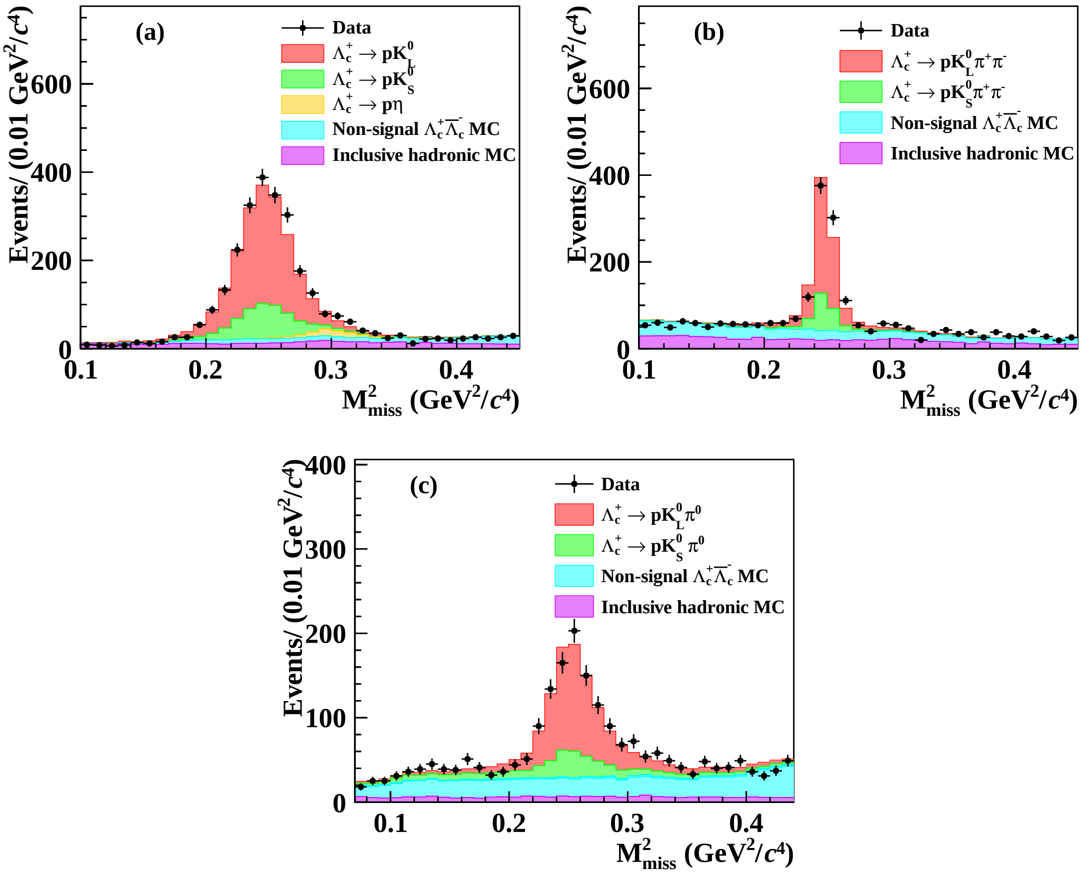

Figure 1. The $M^2_{\rm miss}$ distributions of the selected DT events for (a) $\Lambda_c^+ \to pK_L^0$, (b) $\Lambda_c^+ \to pK_L^0\pi^+\pi^-$, and (c) $\Lambda_c^+ \to pK_L^0\pi^0$ decays. The points with error bars are data combined from seven c.m. energies, the red histograms indicate the signal processes, and the green and orange histograms are the peaking backgrounds. The cyan and violet histograms represent non-signal $\Lambda_c^+\bar{\Lambda}_c^-$ and inclusive hadronic background processes, respectively.

the total number of MC events generated for the i-th tag mode. Table 2 summarizes the contributions arising from each peaking background process.

A simultaneous unbinned maximum-likelihood fit is performed on the $M^2_{\rm miss}$ distributions of the seven c.m. energies. The signal and peaking backgrounds are modeled by individual MC-simulated shapes convolved with Gaussian functions to account for differences between the data and MC simulations. The Gaussian means and widths are free parameters in the fit. The yields of the peaking background events are free with their mean and standard deviation values set to the results listed in Table 2. For the signal mode $\Lambda_c^+ \to pK_L^0\pi^0$, a truth-matching method is employed to obtain the pure signal shape by comparing the two photons from the π^0 with their corresponding MC truth information. The opening angle $\theta_{\rm truth}$ between the truth and the reconstructed photons is required to be less than 10°. The combinatorial background shape is taken from the inclusive MC samples, including non-signal $\Lambda_c^+\bar{\Lambda}_c^-$ and continuum hadron production events.

Table 2. Estimated yields of peaking backgrounds at each c.m. energy. The uncertainties are statistical only.

$\sqrt{s}$ (GeV)	$\Lambda_c^+ \to pK_S^0$	$\Lambda_c^+ \to p\eta$	$\Lambda_c^+ \to pK_S^0\pi^+\pi^-$	$\Lambda_c^+ \to pK_S^0\pi^0$
4.600	59 ± 6	13 ± 1	25 ± 5	44 ± 6
4.612	14 ± 3	2.3± 0.2	4 ± 1	8 ± 3
4.628	70 ± 7	11 ± 1	31 ± 4	38 ± 6
4.641	68 ± 7	12 ± 1	30 ± 5	38 ± 7
4.661	60 ± 6	12 ± 1	39 ± 5	51 ± 8
4.682	198 ± 12	35 ± 3	97 ± 9	150 ± 13
4.699	54 ± 6	10 ± 1	24 ± 5	37 ± 6

The BFs of the decays $\Lambda_c^+ \to pK_L^0$, $\Lambda_c^+ \to pK_L^0\pi^+\pi^-$, and $\Lambda_c^+ \to pK_L^0\pi^0$ are shared variables for the seven c.m. energies in the simultaneous fit, determined by

$$\mathcal{B}_{\rm sig} = \frac{N^{\rm DT}}{N^{\rm ST} \cdot \varepsilon_{\rm avg} \cdot \mathcal{B}_{\rm int}}, \tag{3.5}$$

where $\varepsilon_{\rm avg} = \left(\sum_i N_i^{\rm ST} \cdot \varepsilon_i^{\rm DT}/\varepsilon_i^{\rm ST}\right)/N^{\rm ST}$ is the average detection efficiency for detecting signal modes in ST events and i represents the i-th ST tag mode. Table 3 lists the ST events and the average detection efficiencies for each c.m. energy. $N^{\rm DT}$ and $\varepsilon_i^{\rm DT}$ are the DT yields and corresponding efficiencies, respectively. $\mathcal{B}_{\rm int}$ is the intermediate BF of π^0, $\mathcal{B}(\pi^0 \to \gamma\gamma) = (98.823 \pm 0.034)\%$ [22] for $\Lambda_c^+ \to pK_L^0\pi^0$ decay. Figure 2 shows the results of fits to the $M^2_{\rm miss}$ distributions, combining all data samples. From these fits, the BFs are $\mathcal{B}(\Lambda_c^+ \to pK_L^0) = (1.67 \pm 0.06)\%$, $\mathcal{B}(\Lambda_c^+ \to pK_L^0\pi^+\pi^-) = (1.69 \pm 0.10)\%$, and $\mathcal{B}(\Lambda_c^+ \to pK_L^0\pi^0) = (2.02 \pm 0.13)\%$, where the uncertainties are statistical only. The total DT signal yields from all c.m. energies are $N^{\rm DT}_{pK_L^0} = 1627 \pm 56$, $N^{\rm DT}_{pK_L^0\pi^+\pi^-} = 648 \pm 39$, and $N^{\rm DT}_{pK_L^0\pi^0} = 652 \pm 41$, for $\Lambda_c^+ \to pK_L^0$, $\Lambda_c^+ \to pK_L^0\pi^+\pi^-$, and $\Lambda_c^+ \to pK_L^0\pi^0$, respectively.

Table 3. ST events ($N^{\rm ST}$), average detection efficiencies ($\varepsilon_{\rm avg}$) and DT signal yields ($N^{\rm DT}$) for $\Lambda_c^+ \to pK_L^0$, $\Lambda_c^+ \to pK_L^0\pi^+\pi^-$, and $\Lambda_c^+ \to pK_L^0\pi^0$ decays at each c.m. energy. The errors are statistical only.

	4.600 GeV	4.612 GeV	4.628 GeV	4.641 GeV	4.661 GeV	4.682 GeV	4.698 GeV
$N^{\rm ST}$	17391 ± 171	3114 ± 75	14558 ± 135	15545 ± 165	15235 ± 164	44704 ± 284	12971 ± 158
modes	$\varepsilon_{\rm avg}(\%)$						
$\Lambda_c^+ \to pK_L^0$	76.32 ± 0.08	76.13 ± 0.08	78.12 ± 0.08	78.83 ± 0.08	78.78 ± 0.08	79.66 ± 0.09	79.89 ± 0.09
$\Lambda_c^+ \to pK_L^0\pi^+\pi^-$	28.61 ± 0.16	28.86 ± 0.17	29.87 ± 0.18	30.96 ± 0.17	31.12 ± 0.17	31.93 ± 0.17	32.83 ± 0.18
$\Lambda_c^+ \to pK_L^0\pi^0$	23.83 ± 0.15	24.28 ± 0.15	25.79 ± 0.16	26.40 ± 0.16	26.68 ± 0.16	27.43 ± 0.17	27.27 ± 0.17
modes	$N^{\rm DT}$						
$\Lambda_c^+ \to pK_L^0$	222 ± 8	40 ± 1	190 ± 7	205 ± 7	201 ± 7	596 ± 21	173 ± 6
$\Lambda_c^+ \to pK_L^0\pi^+\pi^-$	84 ± 5	15 ± 1	74 ± 4	81 ± 5	80 ± 5	242 ± 14	72 ± 4
$\Lambda_c^+ \to pK_L^0\pi^0$	83 ± 5	15 ± 1	75 ± 5	82 ± 5	81 ± 5	245 ± 16	71 ± 4

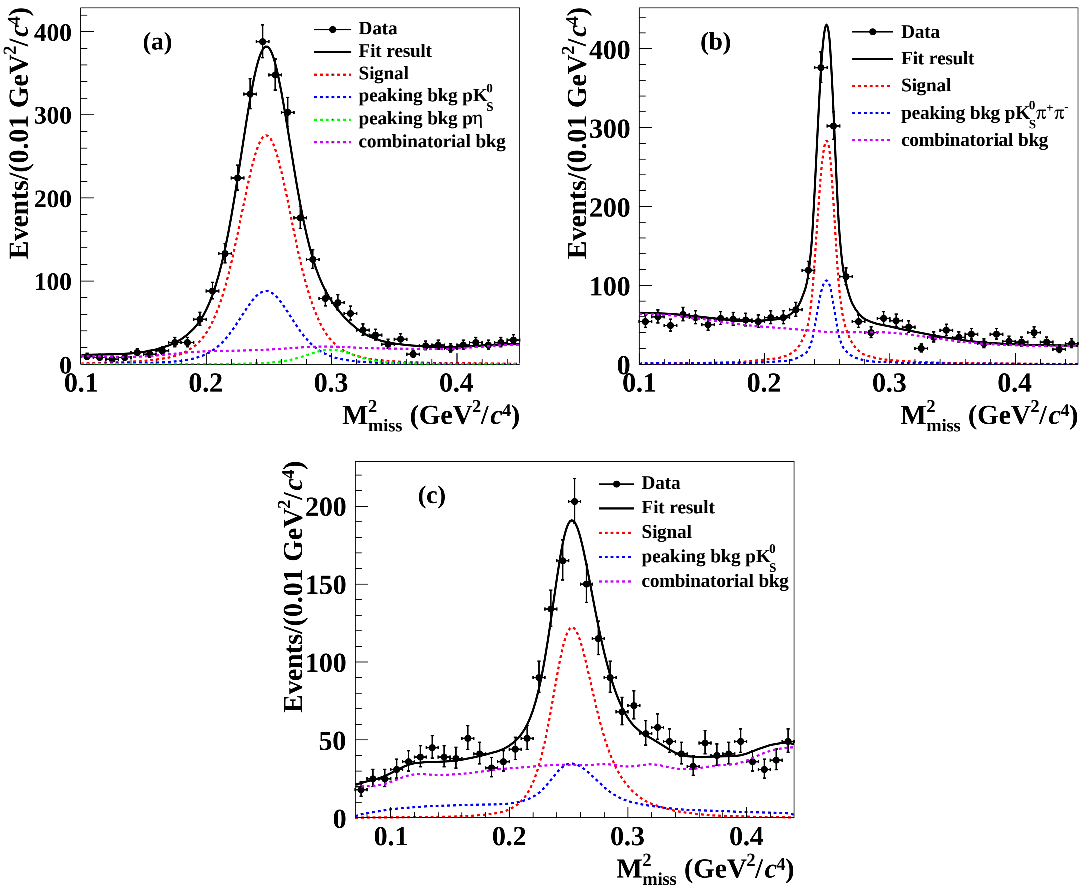

Figure 2. Combined fit results of the $M^2_{\rm miss}$ distributions from all data samples for (a) $\Lambda_c^+ \to pK_L^0$, (b) $\Lambda_c^+ \to pK_L^0\pi^+\pi^-$ and (c) $\Lambda_c^+ \to pK_L^0\pi^0$ decays. The black dots with error bars are data, while the black solid curves are the fit results. The red dashed curves are the signal shapes, and the blue and green dashed curves represent the peaking backgrounds $\Lambda_c^+ \to pK_S^0$ and $\Lambda_c^+ \to p\eta$, respectively. The violet dashed curves are the combinatorial background shapes.

4 Systematic uncertainties

In the DT method, most of the systematic uncertainties associated with the ST selections cancel. The major sources of systematic uncertainties in the BFs measurements are described below and are reported relative to the measured BFs.

- **Tracking and PID efficiencies**. The tracking and PID efficiencies of the charged protons and pions are studied using a control sample of $J/\psi \to p\bar{p}\pi^+\pi^-$ [49]. The MC simulation samples are weighted by the efficiency ratio between data and MC as function of charged particle momentum and $\cos\theta$. The systematic uncertainties of tracking and PID are 0.5% and 0.1% for $\Lambda_c^+ \to pK_L^0$, 1.6% and 0.8% for $\Lambda_c^+ \to pK_L^0\pi^+\pi^-$, and 0.7% and 0.4% for $\Lambda_c^+ \to pK_L^0\pi^0$, respectively.
- **No extra charged track requirement**. The number of good charged tracks is required to be exactly one (three) for pK_L^0 and $pK_L^0\pi^0$ ($pK_L^0\pi^+\pi^-$) DT candidates in

the recoil system of the tagged $\bar{\Lambda}_c^-$. The difference between data and MC simulation from this selection is studied using a control sample of $\Lambda_c^+ \to pK^+\pi^-$. The systematic uncertainty is 1.9%.

- **MC statistics**. The exclusive MC simulation samples are used to obtain the ST and DT detection efficiencies and to estimate the peaking background events. The systematic uncertainties associated with the limited MC sample sizes are estimated to be 0.1%, 0.5%, and 0.5% for $\Lambda_c^+ \to pK_L^0$, $\Lambda_c^+ \to pK_L^0\pi^+\pi^-$, and $\Lambda_c^+ \to pK_L^0\pi^0$, respectively.

- **ST yield**. The systematic uncertainty arising from the total ST yield is assigned to be 0.2% [47].

- **Kinematic fit**. The model of the MC simulation is much simpler than the real detector performance, resulting in a difference between the data and MC simulation in the track parameters of the charged tracks [50]. The helix parameters of the charged tracks are corrected, and the BFs are re-evaluated with the updated MC simulation samples. The differences from the measured BFs are taken as the systematic uncertainties associated with the kinematic fit, which are 0.5%, 1.0%, and 0.5% for $\Lambda_c^+ \to pK_L^0$, $\Lambda_c^+ \to pK_L^0\pi^+\pi^-$ and $\Lambda_c^+ \to pK_L^0\pi^0$, respectively.

- **Angle(γ,$\bar{p}$) requirement**. To estimate the systematic uncertainty of the Angle($\gamma, \bar{p}$) requirement, the difference between the data and MC simulation samples of this requirement is investigated from a control sample of $\psi(3686) \to \pi^+\pi^- J/\psi, J/\psi \to p\bar{p}\pi^0$. The systematic uncertainty is 0.2% for $\Lambda_c^+ \to pK_L^0\pi^0$.

- **π^0 reconstruction**. The systematic uncertainty due to the π^0 reconstruction is determined using the control sample of $J/\psi \to p\bar{p}\pi^0$ [51]. The MC simulation samples are corrected depending on the π^0 momentum. The systematic uncertainty is determined to be 0.5%.

- **Truth-match method**. The systematic uncertainty from the truth-match method is determined comparing the measured BFs with and without the truth-match requirements. The resulting systematic uncertainty is taken as 0.2%.

- **Signal model**. For $\Lambda_c^+ \to pK_L^0$, the systematic uncertainty from the signal model is determined varying the decay asymmetry parameters within $\pm 1\sigma$. The deviation from the measured BF is found to be negligible. For $\Lambda_c^+ \to pK_L^0\pi^+\pi^-$ and $\Lambda_c^+ \to pK_L^0\pi^0$, the signal models in the nominal analysis is tunned based on the data. The possible intermediate resonances are considered in the amplitude analysis, composed of Σ^*, Δ^*, N^*, $\bar{K}^*$ and ρ. The nominal amplitude models are then replaced by alternative ones with equivalent descriptions of the data. The alternative model of $\Lambda_c^+ \to pK_L^0\pi^0$ is selected by removing the insignificant intermediate resonances. For $\Lambda_c^+ \to pK_L^0\pi^+\pi^-$, the amplitude fit is not stable due to the limited statistics of data. An alternative model is chosen with a similar fit quality to the nominal. The systematic uncertainties are determined to be 1.1% and 0.1% for $\Lambda_c^+ \to pK_L^0\pi^+\pi^-$ and $\Lambda_c^+ \to pK_L^0\pi^0$, respectively.

- **Background shape**. To investigate the systematic uncertainty from the background shape, the nominal background shape is replaced with a second-order Chebychev polynomial function in the simultaneous fit. The systematic uncertainties are 0.9%, 0.6%, and 0.4% for $\Lambda_c^+ \to pK_L^0$, $\Lambda_c^+ \to pK_L^0\pi^+\pi^-$ and $\Lambda_c^+ \to pK_L^0\pi^0$, respectively.

- **Fit bias**. The systematic uncertainty from the simultaneous fit is studied with 5000 sets of toy MC samples, which are simulated with all parameters from the fit model fixed. The BFs obtained from the toy samples are fitted with a Gaussian function. The deviations between the Gaussian mean value and nominal BFs are assigned as systematic uncertainties. For the decay $\Lambda_c^+ \to pK_L\pi^0$, the fit bias is found to be 0.27%, while for the other two signal modes it is negligible.

Other sources of systematic uncertainties, such as the BF of $\pi^0 \to \gamma\gamma$, are neglected due to their negligible effects. Assuming that all sources of systematic uncertainties in the BFs measurements are uncorrelated, the quadratic sums of the different sources are considered as the total systematic uncertainties, which are 2.2%, 3.1%, and 2.3% for $\Lambda_c^+ \to pK_L^0$, $\Lambda_c^+ \to pK_L^0\pi^+\pi^-$, and $\Lambda_c^+ \to pK_L^0\pi^0$, respectively. Table 4 lists all the systematic uncertainties discussed above.

Table 4. Relative systematic uncertainties in the BF measurements.

Source	$\Lambda_c^+ \to pK_L^0$ (%)	$\Lambda_c^+ \to pK_L^0\pi^+\pi^-$ (%)	$\Lambda_c^+ \to pK_L^0\pi^0$ (%)
Tracking	0.5	1.6	0.7
PID	0.1	0.8	0.4
No extra charged track	1.9	1.9	1.9
MC statistics	0.2	0.5	0.5
ST yields	0.2	0.2	0.2
Kinematic fit	0.5	1.0	0.5
Angle(γ,$\bar{p}$) requirement	-	-	0.2
π^0 reconstruction	-	-	0.5
Truth-match method	-	-	0.2
Signal model	-	1.1	0.1
Background shape	0.9	0.6	0.4
Fit bias	-	-	0.3
Total	2.2	3.1	2.3

5 Summary

In summary, we report the BFs of $\Lambda_c^+ \to pK_L^0$, $\Lambda_c^+ \to pK_L^0\pi^+\pi^-$ and $\Lambda_c^+ \to pK_L^0\pi^0$ for the first time, by analyzing e^+e^- annihilation data samples corresponding to an integrated luminosity of 4.5 fb^{-1} collected at c.m. energies between 4.600 and 4.699 GeV. The measured BFs of these decays are $\mathcal{B}(\Lambda_c^+ \to pK_L^0) = (1.67 \pm 0.06 \pm 0.04)\%$, $\mathcal{B}(\Lambda_c^+ \to$

$pK_L^0\pi^+\pi^-) = (1.69 \pm 0.10 \pm 0.05)\%$, and $\mathcal{B}(\Lambda_c^+ \to pK_L^0\pi^0) = (2.02 \pm 0.13 \pm 0.05)\%$. Combining the BFs measurements in this work with the values of $\mathcal{B}(\Lambda_c^+ \to K_S^0 X)$ [22], the K_S^0-K_L^0 asymmetries are determined, as summarized in Table 5. The uncertainties are derived through the standard error propagation procedure, assuming that the uncertainties of the estimated $\mathcal{B}(\Lambda_c^+ \to K_L^0 X)$ and the quoted $\mathcal{B}(\Lambda_c^+ \to K_S^0 X)$ are uncorrelated. Taking into account the uncertainties, no obvious asymmetry is observed in any of the three decays. The K_S^0-K_L^0 asymmetry of $\Lambda_c^+ \to pK_{S,L}^0$ $R(\Lambda_c^+, pK_{S,L}^0) = -0.025 \pm 0.031$ is compatible with the prediction of $(-0.010, 0.087)$ based on SU(3) flavor symmetry [18]. Our measurements of the K_S^0-K_L^0 asymmetries in charmed baryon decays offer the possibility to access the DCS processes involving neutral kaons and provide further constraints on their amplitudes.

Table 5. The BFs $\mathcal{B}(\Lambda_c^+ \to K_L^0 X)$, the known BFs $\mathcal{B}(\Lambda_c^+ \to K_S^0 X)$, and K_S^0-K_L^0 asymmetries.

Mode	$\mathcal{B}(\Lambda_c^+ \to K_L^0 X)$ (%)	$\mathcal{B}(\Lambda_c^+ \to K_S^0 X)$ (%) [22]	$R(\Lambda_c^+, K_{L,S}^0 X)$
$\Lambda_c^+ \to pK_{L,S}^0$	1.67 ± 0.06 ± 0.04	1.59 ± 0.07	-0.025 ± 0.031
$\Lambda_c^+ \to pK_{L,S}^0\pi^+\pi^-$	1.69 ± 0.10 ± 0.05	1.60 ± 0.11	-0.027 ± 0.048
$\Lambda_c^+ \to pK_{L,S}^0\pi^0$	2.02 ± 0.13 ± 0.05	1.96 ± 0.12	-0.015 ± 0.046

Acknowledgments

The BESIII Collaboration thanks the staff of BEPCII and the IHEP computing center for their strong support. This work is supported in part by National Key R&D Program of China under Contracts Nos. 2020YFA0406400, 2020YFA0406300, 2023YFA1606000; National Natural Science Foundation of China (NSFC) under Contracts Nos. 11635010, 11735014, 11935015, 11935016, 11935018, 12025502, 12035009, 12035013, 12061131003, 12192260, 12192261, 12192262, 12192263, 12192264, 12192265, 12221005, 12225509, 12235017, 12361141819; the Chinese Academy of Sciences (CAS) Large-Scale Scientific Facility Program; the CAS Center for Excellence in Particle Physics (CCEPP); Joint Large-Scale Scientific Facility Funds of the NSFC and CAS under Contract No. U1832207; 100 Talents Program of CAS; The Institute of Nuclear and Particle Physics (INPAC) and Shanghai Key Laboratory for Particle Physics and Cosmology; German Research Foundation DFG under Contracts Nos. 455635585, FOR5327, GRK 2149; Istituto Nazionale di Fisica Nucleare, Italy; Ministry of Development of Turkey under Contract No. DPT2006K-120470; National Research Foundation of Korea under Contract No. NRF-2022R1A2C1092335; National Science and Technology fund of Mongolia; National Science Research and Innovation Fund (NSRF) via the Program Management Unit for Human Resources & Institutional Development, Research and Innovation of Thailand under Contract No. B16F640076; Polish National Science Centre under Contract No. 2019/35/O/ST2/02907; The Swedish Research Council; U. S. Department of Energy under Contract No. DE-FG02-05ER41374

References

[1] H.-Y. Cheng, *Charmed baryon physics circa 2021*, *Chin. J. Phys.* **78** (2022) 324 [arXiv:2109.01216].

[2] J.G. Korner and M. Kramer, *Exclusive nonleptonic charm baryon decays*, *Z. Phys. C* **55** (1992) 659.

[3] M.A. Ivanov, J.G. Korner, V.E. Lyubovitskij and A.G. Rusetsky, *Exclusive nonleptonic decays of bottom and charm baryons in a relativistic three quark model: Evaluation of nonfactorizing diagrams*, *Phys. Rev. D* **57** (1998) 5632 [hep-ph/9709372].

[4] H.-Y. Cheng and B. Tseng, *Nonleptonic weak decays of charmed baryons*, *Phys. Rev. D* **46** (1992) 1042.

[5] Q.P. Xu and A.N. Kamal, *Cabibbo favored nonleptonic decays of charmed baryons*, *Phys. Rev. D* **46** (1992) 270.

[6] H.-Y. Cheng and B. Tseng, *Cabibbo allowed nonleptonic weak decays of charmed baryons*, *Phys. Rev. D* **48** (1993) 4188 [hep-ph/9304286].

[7] Q.P. Xu and A.N. Kamal, *The Nonleptonic charmed baryon decays: $B_c \to B(\frac{3}{2}^+, \text{decuplet}) + P(0^-)$ or $V(1^-)$*, *Phys. Rev. D* **46** (1992) 3836.

[8] P. Zenczykowski, *Nonleptonic charmed baryon decays: Symmetry properties of parity violating amplitudes*, *Phys. Rev. D* **50** (1994) 5787.

[9] K.K. Sharma and R.C. Verma, *A Study of weak mesonic decays of Λ_c and Ξ_c baryons on the basis of HQET results*, *Eur. Phys. J. C* **7** (1999) 217 [hep-ph/9803302].

[10] J.G. Körner, G. Kramer and J. Willrodt, *Weak Decays of the Charmed Baryon C_0^+ and the Inclusive Yield of Λ and p*, *Phys. Lett. B* **78** (1978) 492.

[11] T. Uppal, R.C. Verma and M.P. Khanna, *Constituent quark model analysis of weak mesonic decays of charm baryons*, *Phys. Rev. D* **49** (1994) 3417.

[12] C.-D. Lü, W. Wang and F.-S. Yu, *Test flavor SU(3) symmetry in exclusive Λ_c decays*, *Phys. Rev. D* **93** (2016) 056008 [arXiv:1601.04241].

[13] M.J. Savage and R.P. Springer, *SU(3) Predictions for Charmed Baryon Decays*, *Phys. Rev. D* **42** (1990) 1527.

[14] Y. Kohara, *Quark diagram analysis of charmed baryon decays*, *Phys. Rev. D* **44** (1991) 2799.

[15] R.C. Verma and M.P. Khanna, *Cabibbo favored hadronic decays of charmed baryons in flavor SU(3)*, *Phys. Rev. D* **53** (1996) 3723 [hep-ph/9506394].

[16] L.-L. Chau, H.-Y. Cheng and B. Tseng, *Analysis of two-body decays of charmed baryons using the quark diagram scheme*, *Phys. Rev. D* **54** (1996) 2132 [hep-ph/9508382].

[17] I.I.Y. Bigi and H. Yamamoto, *Interference between Cabibbo allowed and doubly forbidden transitions in $D \to K_{S,L} + \pi' s$ decays*, *Phys. Lett. B* **349** (1995) 363 [hep-ph/9502238].

[18] D. Wang, P.-F. Guo, W.-H. Long and F.-S. Yu, *K^0_S-K^0_L asymmetries and CP violation in charmed baryon decays into neutral kaons*, *JHEP* **03** (2018) 066 [arXiv:1709.09873].

[19] CLEO collaboration, *Comparison of $D \to K^0_S\pi$ and $D \to K^0_L\pi$ Decay Rates*, *Phys. Rev. Lett.* **100** (2008) 091801 [arXiv:0711.1463].

[20] BESIII collaboration, *Measurements of absolute branching fractions of $D^0 \to K^0_L\phi$, $K^0_L\eta$, $K^0_L\omega$, and $K^0_L\eta'$*, *Phys. Rev. D* **105** (2022) 092010 [arXiv:2202.13601].

[21] BESIII collaboration, *Study of the Decays $D_s^+ \to K_S^0 K^+$ and $K_L^0 K^+$*, Phys. Rev. D **99** (2019) 112005 [arXiv:1903.04164].

[22] Particle Data Group collaboration, *Review of Particle Physics*, PTEP **2022** (2022) 083C01.

[23] BESIII collaboration, *Measurement of integrated luminosities at BESIII for data samples at center-of-mass energies between 4.0 and 4.6 GeV*, Chin. Phys. C **46** (2022) 113002 [arXiv:2203.03133].

[24] BESIII collaboration, *Luminosities and energies of e^+e^- collision data taken between $\sqrt{s}$=4.61 GeV and 4.95 GeV at BESIII*, Chin. Phys. C **46** (2022) 113003 [arXiv:2205.04809].

[25] BESIII collaboration, *Design and Construction of the BESIII Detector*, Nucl. Instrum. Meth. A **614** (2010) 345 [arXiv:0911.4960].

[26] C. Yu et al., *BEPCII Performance and Beam Dynamics Studies on Luminosity*, in *7th International Particle Accelerator Conference*, p. TUYA01, 2016, DOI.

[27] BESIII collaboration, *Future Physics Programme of BESIII*, Chin. Phys. C **44** (2020) 040001 [arXiv:1912.05983].

[28] K.-X. Huang, Z.-J. Li, Z. Qian, J. Zhu, H.-Y. Li, Y.-M. Zhang et al., *Method for detector description transformation to Unity and application in BESIII*, Nucl. Sci. Tech. **33** (2022) 142 [arXiv:2206.10117].

[29] X. Li et al., *Study of MRPC technology for BESIII endcap-TOF upgrade*, Radiat. Detect. Technol. Methods **1** (2017) 13.

[30] Y.-X. Guo et al., *The study of time calibration for upgraded end cap TOF of BESIII*, Radiat. Detect. Technol. Methods **1** (2017) 15.

[31] D.J. Lange, *The EvtGen particle decay simulation package*, Nucl. Instrum. Meth. A **462** (2001) 152.

[32] GEANT4 collaboration, *GEANT4–a simulation toolkit*, Nucl. Instrum. Meth. A **506** (2003) 250.

[33] Y. Zheng-Yun, L. Yu-Tie and M. Ya-Jun, *A method for detector description exchange among ROOT GEANT4 and GEANT3*, Chin. Phys. C **32** (2008) 572.

[34] Y.-T. Liang et al., *A uniform geometry description for simulation, reconstruction and visualization in the BESIII experiment*, Nucl. Instrum. Meth. A **603** (2009) 325.

[35] S. Jadach, B.F.L. Ward and Z. Was, *Coherent exclusive exponentiation for precision Monte Carlo calculations*, Phys. Rev. D **63** (2001) 113009 [hep-ph/0006359].

[36] S. Jadach, B.F.L. Ward and Z. Was, *The Precision Monte Carlo event generator K K for two fermion final states in e^+e^- collisions*, Comput. Phys. Commun. **130** (2000) 260 [hep-ph/9912214].

[37] R.-G. Ping, *Event generators at BESIII*, Chin. Phys. C **32** (2008) 599.

[38] J.C. Chen, G.S. Huang, X.R. Qi, D.H. Zhang and Y.S. Zhu, *Event generator for J/ψ and $\psi(2S)$ decay*, Phys. Rev. D **62** (2000) 034003.

[39] E. Richter-Was, *QED bremsstrahlung in semileptonic B and leptonic tau decays*, Phys. Lett. B **303** (1993) 163.

[40] BESIII collaboration, *Precision measurement of the $e^+e^- \rightarrow \Lambda_c^+\bar{\Lambda}_c^-$ cross section near threshold*, Phys. Rev. Lett. **120** (2018) 132001 [arXiv:1710.00150].

[41] BESIII collaboration, *Measurement of Energy-Dependent Pair-Production Cross Section and Electromagnetic Form Factors of a Charmed Baryon*, Phys. Rev. Lett. **131** (2023) 191901 [arXiv:2307.07316].

[42] BESIII collaboration, *Measurements of Weak Decay Asymmetries of $\Lambda_c^+ \rightarrow pK_S^0$, $\Lambda\pi^+$, $\Sigma^+\pi^0$, and $\Sigma^0\pi^+$*, Phys. Rev. D **100** (2019) 072004 [arXiv:1905.04707].

[43] MARK-III collaboration, *Direct Measurements of Charmed D Meson Hadronic Branching Fractions*, Phys. Rev. Lett. **56** (1986) 2140.

[44] MARK-III collaboration, *A Reanalysis of Charmed D Meson Branching Fractions*, .

[45] B.-C. Ke, J. Koponen, H.-B. Li and Y. Zheng, *Recent Progress in Leptonic and Semileptonic Decays of Charmed Hadrons*, Ann. Rev. Nucl. Part. Sci. **73** (2023) 285 [arXiv:2310.05228].

[46] H.-B. Li and X.-R. Lyu, *Study of the standard model with weak decays of charmed hadrons at BESIII*, Natl. Sci. Rev. **8** (2021) nwab181 [2103.00908].

[47] BESIII collaboration, *Observations of the Cabibbo-Suppressed decays $\Lambda_c^+ \rightarrow n\pi^+\pi^0$, $n\pi^+\pi^-\pi^+$ and the Cabibbo-Favored decay $\Lambda_c^+ \rightarrow nK^-\pi^+\pi^+$*, Chin. Phys. C **47** (2023) 023001 [arXiv:2210.03375].

[48] BESIII collaboration, *Measurements of absolute hadronic branching fractions of Λ_c^+ baryon*, Phys. Rev. Lett. **116** (2016) 052001 [arXiv:1511.08380].

[49] BESIII collaboration, *Observation of the Singly Cabibbo Suppressed Decay $\Lambda_c^+ \rightarrow n\pi^+$*, Phys. Rev. Lett. **128** (2022) 142001 [arXiv:2201.02056].

[50] BESIII collaboration, *Search for hadronic transition $\chi_{cj} \rightarrow \eta_c\pi^+\pi^-$ and observation of $\chi_{cj} \rightarrow K\overline{K}\pi\pi\pi$*, Phys. Rev. D **87** (2013) 012002 [arXiv:1208.4805].

[51] BESIII collaboration, *Observation of the J/ψ and $\psi(3686)$ decays into $\eta\Sigma^+\Sigma^-$*, Phys. Rev. D **106** (2022) 112007 [arXiv:2210.09601].

The BESIII collaboration

M. Ablikim[1], M. N. Achasov[4,c], P. Adlarson[76], O. Afedulidis[3], X. C. Ai[81], R. Aliberti[35], A. Amoroso[75A,75C], Q. An[72,58,a], Y. Bai[57], O. Bakina[36], I. Balossino[29A], Y. Ban[46,h], H.-R. Bao[64], V. Batozskaya[1,44], K. Begzsuren[32], N. Berger[35], M. Berlowski[44], M. Bertani[28A], D. Bettoni[29A], F. Bianchi[75A,75C], E. Bianco[75A,75C], A. Bortone[75A,75C], I. Boyko[36], R. A. Briere[5], A. Brueggemann[69], H. Cai[77], X. Cai[1,58], A. Calcaterra[28A], G. F. Cao[1,64], N. Cao[1,64], S. A. Cetin[62A], J. F. Chang[1,58], G. R. Che[43], G. Chelkov[36,b], C. Chen[43], C. H. Chen[9], Chao Chen[55], G. Chen[1], H. S. Chen[1,64], H. Y. Chen[20], M. L. Chen[1,58,64], S. J. Chen[42], S. L. Chen[45], S. M. Chen[61], T. Chen[1,64], X. R. Chen[31,64], X. T. Chen[1,64], Y. B. Chen[1,58], Y. Q. Chen[34], Z. J. Chen[25,i], Z. Y. Chen[1,64], S. K. Choi[10], G. Cibinetto[29A], F. Cossio[75C], J. J. Cui[50], H. L. Dai[1,58], J. P. Dai[79], A. Dbeyssi[18], R. E. de Boer[3], D. Dedovich[36], C. Q. Deng[73], Z. Y. Deng[1], A. Denig[35], I. Denysenko[36], M. Destefanis[75A,75C], F. De Mori[75A,75C], B. Ding[67,1], X. X. Ding[46,h], Y. Ding[40], Y. Ding[34], J. Dong[1,58], L. Y. Dong[1,64], M. Y. Dong[1,58,64], X. Dong[77], M. C. Du[1], S. X. Du[81], Y. Y. Duan[55], Z. H. Duan[42], P. Egorov[36,b], Y. H. Fan[45], J. Fang[59], J. Fang[1,58], S. S. Fang[1,64], W. X. Fang[1], Y. Fang[1], Y. Q. Fang[1,58], R. Farinelli[29A], L. Fava[75B,75C], F. Feldbauer[3], G. Felici[28A], C. Q. Feng[72,58], J. H. Feng[59], Y. T. Feng[72,58], M. Fritsch[3], C. D. Fu[1], J. L. Fu[64], Y. W. Fu[1,64], H. Gao[64], X. B. Gao[41], Y. N. Gao[46,h], Yang Gao[72,58], S. Garbolino[75C], I. Garzia[29A,29B], L. Ge[81], P. T. Ge[19], Z. W. Ge[42], C. Geng[59], E. M. Gersabeck[68], A. Gilman[70], K. Goetzen[13], L. Gong[40], W. X. Gong[1,58], W. Gradl[35], S. Gramigna[29A,29B], M. Greco[75A,75C], M. H. Gu[1,58], Y. T. Gu[15], C. Y. Guan[1,64], A. Q. Guo[31,64], L. B. Guo[41], M. J. Guo[50], R. P. Guo[49], Y. P. Guo[12,g], A. Guskov[36,b], J. Gutierrez[27], K. L. Han[64], T. T. Han[1], F. Hanisch[3], X. Q. Hao[19], F. A. Harris[66], K. K. He[55], K. L. He[1,64], F. H. Heinsius[3], C. H. Heinz[35], Y. K. Heng[1,58,64], C. Herold[60], T. Holtmann[3], P. C. Hong[34], G. Y. Hou[1,64], X. T. Hou[1,64], Y. R. Hou[64], Z. L. Hou[1], B. Y. Hu[59], H. M. Hu[1,64], J. F. Hu[56,j], S. L. Hu[12,g], T. Hu[1,58,64], Y. Hu[1], G. S. Huang[72,58], K. X. Huang[59], L. Q. Huang[31,64], X. T. Huang[50], Y. P. Huang[1], Y. S. Huang[59], T. Hussain[74], F. Hölzken[3], N. Hüsken[35], N. in der Wiesche[69], J. Jackson[27], S. Janchiv[32], J. H. Jeong[10], Q. Ji[1], Q. P. Ji[19], W. Ji[1,64], X. B. Ji[1,64], X. L. Ji[1,58], Y. Y. Ji[50], X. Q. Jia[50], Z. K. Jia[72,58], D. Jiang[1,64], H. B. Jiang[77], P. C. Jiang[46,h], S. S. Jiang[39], T. J. Jiang[16], X. S. Jiang[1,58,64], Y. Jiang[64], J. B. Jiao[50], J. K. Jiao[34], Z. Jiao[23], S. Jin[42], Y. Jin[67], M. Q. Jing[1,64], X. M. Jing[64], T. Johansson[76], S. Kabana[33], N. Kalantar-Nayestanaki[65], X. L. Kang[9], X. S. Kang[40], M. Kavatsyuk[65], B. C. Ke[81], V. Khachatryan[27], A. Khoukaz[69], R. Kiuchi[1], O. B. Kolcu[62A], B. Kopf[3], M. Kuessner[3], X. Kui[1,64], N. Kumar[26], A. Kupsc[44,76], W. Kühn[37], J. J. Lane[68], L. Lavezzi[75A,75C], T. T. Lei[72,58], Z. H. Lei[72,58], M. Lellmann[35], T. Lenz[35], C. Li[47], C. Li[43], C. H. Li[39], Cheng Li[72,58], D. M. Li[81], F. Li[1,58], G. Li[1], H. B. Li[1,64], H. J. Li[19], H. N. Li[56,j], Hui Li[43], J. R. Li[61], J. S. Li[59], K. Li[1], K. L. Li[19], L. J. Li[1,64], L. K. Li[1], Lei Li[48], M. H. Li[43], P. R. Li[38,k,l], Q. M. Li[1,64], Q. X. Li[50], R. Li[17,31], S. X. Li[12], T. Li[50], W. D. Li[1,64], W. G. Li[1,a], X. Li[1,64], X. H. Li[72,58], X. L. Li[50], X. Y. Li[1,64], X. Z. Li[59], Y. G. Li[46,h], Z. J. Li[59], Z. Y. Li[79], C. Liang[42], H. Liang[1,64], H. Liang[72,58], Y. F. Liang[54], Y. T. Liang[31,64], G. R. Liao[14], Y. P. Liao[1,64], J. Libby[26], A. Limphirat[60], C. C. Lin[55], D. X. Lin[31,64], T. Lin[1], B. J. Liu[1], B. X. Liu[77], C. Liu[34], C. X. Liu[1], F. Liu[1], F. H. Liu[53], Feng Liu[6], G. M. Liu[56,j], H. Liu[38,k,l], H. B. Liu[15], H. H. Liu[1], H. M. Liu[1,64], Huihui Liu[21], J. B. Liu[72,58], J. Y. Liu[1,64], K. Liu[38,k,l], K. Y. Liu[40], Ke Liu[22], L. Liu[72,58], L. C. Liu[43], Lu Liu[43], M. H. Liu[12,g], P. L. Liu[1], Q. Liu[64], S. B. Liu[72,58], T. Liu[12,g], W. K. Liu[43], W. M. Liu[72,58], X. Liu[38,k,l], X. Liu[39], Y. Liu[81], Y. Liu[38,k,l], Y. B. Liu[43], Z. A. Liu[1,58,64], Z. D. Liu[9], Z. Q. Liu[50], X. C. Lou[1,58,64], F. X. Lu[59], H. J. Lu[23], J. G. Lu[1,58], X. L. Lu[1], Y. Lu[7], Y. P. Lu[1,58], Z. H. Lu[1,64], C. L. Luo[41], J. R. Luo[59], M. X. Luo[80], T. Luo[12,g], X. L. Luo[1,58], X. R. Lyu[64], Y. F. Lyu[43], F. C. Ma[40], H. Ma[79], H. L. Ma[1], J. L. Ma[1,64], L. L. Ma[50], L. R. Ma[67], M. M. Ma[1,64], Q. M. Ma[1], R. Q. Ma[1,64],

T. Ma[72,58], X. T. Ma[1,64], X. Y. Ma[1,58], Y. Ma[46,h], Y. M. Ma[31], F. E. Maas[18], M. Maggiora[75A,75C], S. Malde[70], Y. J. Mao[46,h], Z. P. Mao[1], S. Marcello[75A,75C], Z. X. Meng[67], J. G. Messchendorp[13,65], G. Mezzadri[29A], H. Miao[1,64], T. J. Min[42], R. E. Mitchell[27], X. H. Mo[1,58,64], B. Moses[27], N. Yu. Muchnoi[4,c], J. Muskalla[35], Y. Nefedov[36], F. Nerling[18,e], L. S. Nie[20], I. B. Nikolaev[4,c], Z. Ning[1,58], S. Nisar[11,m], Q. L. Niu[38,k,l], W. D. Niu[55], Y. Niu [50], S. L. Olsen[64], Q. Ouyang[1,58,64], S. Pacetti[28B,28C], X. Pan[55], Y. Pan[57], A. Pathak[34], Y. P. Pei[72,58], M. Pelizaeus[3], H. P. Peng[72,58], Y. Y. Peng[38,k,l], K. Peters[13,e], J. L. Ping[41], R. G. Ping[1,64], S. Plura[35], V. Prasad[33], F. Z. Qi[1], H. Qi[72,58], H. R. Qi[61], M. Qi[42], T. Y. Qi[12,g], S. Qian[1,58], W. B. Qian[64], C. F. Qiao[64], X. K. Qiao[81], J. J. Qin[73], L. Q. Qin[14], L. Y. Qin[72,58], X. P. Qin[12,g], X. S. Qin[50], Z. H. Qin[1,58], J. F. Qiu[1], Z. H. Qu[73], C. F. Redmer[35], K. J. Ren[39], A. Rivetti[75C], M. Rolo[75C], G. Rong[1,64], Ch. Rosner[18], S. N. Ruan[43], N. Salone[44], A. Sarantsev[36,d], Y. Schelhaas[35], K. Schoenning[76], M. Scodeggio[29A], K. Y. Shan[12,g], W. Shan[24], X. Y. Shan[72,58], Z. J. Shang[38,k,l], J. F. Shangguan[16], L. G. Shao[1,64], M. Shao[72,58], C. P. Shen[12,g], H. F. Shen[1,8], W. H. Shen[64], X. Y. Shen[1,64], B. A. Shi[64], H. Shi[72,58], H. C. Shi[72,58], J. L. Shi[12,g], J. Y. Shi[1], Q. Q. Shi[55], S. Y. Shi[73], X. Shi[1,58], J. J. Song[19], T. Z. Song[59], W. M. Song[34,1], Y. J. Song[12,g], Y. X. Song[46,h,n], S. Sosio[75A,75C], S. Spataro[75A,75C], F. Stieler[35], S. S Su[40], Y. J. Su[64], G. B. Sun[77], G. X. Sun[1], H. Sun[64], H. K. Sun[1], J. F. Sun[19], K. Sun[61], L. Sun[77], S. S. Sun[1,64], T. Sun[51,f], W. Y. Sun[34], Y. Sun[9], Y. J. Sun[72,58], Y. Z. Sun[1], Z. Q. Sun[1,64], Z. T. Sun[50], C. J. Tang[54], G. Y. Tang[1], J. Tang[59], M. Tang[72,58], Y. A. Tang[77], L. Y. Tao[73], Q. T. Tao[25,i], M. Tat[70], J. X. Teng[72,58], V. Thoren[76], W. H. Tian[59], Y. Tian[31,64], Z. F. Tian[77], I. Uman[62B], Y. Wan[55], S. J. Wang [50], B. Wang[1], B. L. Wang[64], Bo Wang[72,58], D. Y. Wang[46,h], F. Wang[73], H. J. Wang[38,k,l], J. J. Wang[77], J. P. Wang [50], K. Wang[1,58], L. L. Wang[1], M. Wang[50], N. Y. Wang[64], S. Wang[12,g], S. Wang[38,k,l], T. Wang[12,g], T. J. Wang[43], W. Wang[73], W. Wang[59], W. P. Wang[35,58,72,o], X. Wang[46,h], X. F. Wang[38,k,l], X. J. Wang[39], X. L. Wang[12,g], X. N. Wang[1], Y. Wang[61], Y. D. Wang[45], Y. F. Wang[1,58,64], Y. L. Wang[19], Y. N. Wang[45], Y. Q. Wang[1], Yaqian Wang[17], Yi Wang[61], Z. Wang[1,58], Z. L. Wang[73], Z. Y. Wang[1,64], Ziyi Wang[64], D. H. Wei[14], F. Weidner[69], S. P. Wen[1], Y. R. Wen[39], U. Wiedner[3], G. Wilkinson[70], M. Wolke[76], L. Wollenberg[3], C. Wu[39], J. F. Wu[1,8], L. H. Wu[1], L. J. Wu[1,64], X. Wu[12,g], X. H. Wu[34], Y. Wu[72,58], Y. H. Wu[55], Y. J. Wu[31], Z. Wu[1,58], L. Xia[72,58], X. M. Xian[39], B. H. Xiang[1,64], T. Xiang[46,h], D. Xiao[38,k,l], G. Y. Xiao[42], S. Y. Xiao[1], Y. L. Xiao[12,g], Z. J. Xiao[41], C. Xie[42], X. H. Xie[46,h], Y. Xie[50], Y. G. Xie[1,58], Y. H. Xie[6], Z. P. Xie[72,58], T. Y. Xing[1,64], C. F. Xu[1,64], C. J. Xu[59], G. F. Xu[1], H. Y. Xu[67,2,p], M. Xu[72,58], Q. J. Xu[16], Q. N. Xu[30], W. Xu[1], W. L. Xu[67], X. P. Xu[55], Y. Xu[40], Y. C. Xu[78], Z. S. Xu[64], F. Yan[12,g], L. Yan[12,g], W. B. Yan[72,58], W. C. Yan[81], X. Q. Yan[1,64], H. J. Yang[51,f], H. L. Yang[34], H. X. Yang[1], T. Yang[1], Y. Yang[12,g], Y. F. Yang[43], Y. F. Yang[1,64], Y. X. Yang[1,64], Z. W. Yang[38,k,l], Z. P. Yao[50], M. Ye[1,58], M. H. Ye[8], J. H. Yin[1], Junhao Yin[43], Z. Y. You[59], B. X. Yu[1,58,64], C. X. Yu[43], G. Yu[1,64], J. S. Yu[25,i], M. C. Yu[40], T. Yu[73], X. D. Yu[46,h], Y. C. Yu[81], C. Z. Yuan[1,64], J. Yuan[34], J. Yuan[45], L. Yuan[2], S. C. Yuan[1,64], Y. Yuan[1,64], Z. Y. Yuan[59], C. X. Yue[39], A. A. Zafar[74], F. R. Zeng[50], S. H. Zeng[63A,63B,63C,63D], X. Zeng[12,g], Y. Zeng[25,i], Y. J. Zeng[59], Y. J. Zeng[1,64], X. Y. Zhai[34], Y. C. Zhai[50], Y. H. Zhan[59], A. Q. Zhang[1,64], B. L. Zhang[1,64], B. X. Zhang[1], D. H. Zhang[43], G. Y. Zhang[19], H. Zhang[72,58], H. Zhang[81], H. C. Zhang[1,58,64], H. H. Zhang[59], H. H. Zhang[34], H. Q. Zhang[1,58,64], H. R. Zhang[72,58], H. Y. Zhang[1,58], J. Zhang[81], J. Zhang[59], J. J. Zhang[52], J. L. Zhang[20], J. Q. Zhang[41], J. S. Zhang[12,g], J. W. Zhang[1,58,64], J. X. Zhang[38,k,l], J. Y. Zhang[1], J. Z. Zhang[1,64], Jianyu Zhang[64], L. M. Zhang[61], Lei Zhang[42], P. Zhang[1,64], Q. Y. Zhang[34], R. Y. Zhang[38,k,l], S. H. Zhang[1,64], Shulei Zhang[25,i], X. D. Zhang[45], X. M. Zhang[1], X. Y Zhang[40], X. Y. Zhang[50], Y. Zhang[73], Y. Zhang[1], Y. T. Zhang[81], Y. H. Zhang[1,58], Y. M. Zhang[39], Yan Zhang[72,58], Z. D. Zhang[1], Z. H. Zhang[1], Z. L. Zhang[34], Z. Y. Zhang[77], Z. Y. Zhang[43], Z. Z. Zhang[45], G. Zhao[1], J. Y. Zhao[1,64], J. Z. Zhao[1,58], L. Zhao[1], Lei Zhao[72,58], M. G. Zhao[43],

N. Zhao[79], R. P. Zhao[64], S. J. Zhao[81], Y. B. Zhao[1,58], Y. X. Zhao[31,64], Z. G. Zhao[72,58], A. Zhemchugov[36,b], B. Zheng[73], B. M. Zheng[34], J. P. Zheng[1,58], W. J. Zheng[1,64], Y. H. Zheng[64], B. Zhong[41], X. Zhong[59], H. Zhou[50], J. Y. Zhou[34], L. P. Zhou[1,64], S. Zhou[6], X. Zhou[77], X. K. Zhou[6], X. R. Zhou[72,58], X. Y. Zhou[39], Y. Z. Zhou[12,g], Z. C. Zhou[20], A. N. Zhu[64], J. Zhu[43], K. Zhu[1], K. J. Zhu[1,58,64], K. S. Zhu[12,g], L. Zhu[34], L. X. Zhu[64], S. H. Zhu[71], T. J. Zhu[12,g], W. D. Zhu[41], Y. C. Zhu[72,58], Z. A. Zhu[1,64], J. H. Zou[1], J. Zu[72,58]

(BESIII Collaboration)

[1] *Institute of High Energy Physics, Beijing 100049, People's Republic of China*
[2] *Beihang University, Beijing 100191, People's Republic of China*
[3] *Bochum Ruhr-University, D-44780 Bochum, Germany*
[4] *Budker Institute of Nuclear Physics SB RAS (BINP), Novosibirsk 630090, Russia*
[5] *Carnegie Mellon University, Pittsburgh, Pennsylvania 15213, USA*
[6] *Central China Normal University, Wuhan 430079, People's Republic of China*
[7] *Central South University, Changsha 410083, People's Republic of China*
[8] *China Center of Advanced Science and Technology, Beijing 100190, People's Republic of China*
[9] *China University of Geosciences, Wuhan 430074, People's Republic of China*
[10] *Chung-Ang University, Seoul, 06974, Republic of Korea*
[11] *COMSATS University Islamabad, Lahore Campus, Defence Road, Off Raiwind Road, 54000 Lahore, Pakistan*
[12] *Fudan University, Shanghai 200433, People's Republic of China*
[13] *GSI Helmholtzcentre for Heavy Ion Research GmbH, D-64291 Darmstadt, Germany*
[14] *Guangxi Normal University, Guilin 541004, People's Republic of China*
[15] *Guangxi University, Nanning 530004, People's Republic of China*
[16] *Hangzhou Normal University, Hangzhou 310036, People's Republic of China*
[17] *Hebei University, Baoding 071002, People's Republic of China*
[18] *Helmholtz Institute Mainz, Staudinger Weg 18, D-55099 Mainz, Germany*
[19] *Henan Normal University, Xinxiang 453007, People's Republic of China*
[20] *Henan University, Kaifeng 475004, People's Republic of China*
[21] *Henan University of Science and Technology, Luoyang 471003, People's Republic of China*
[22] *Henan University of Technology, Zhengzhou 450001, People's Republic of China*
[23] *Huangshan College, Huangshan 245000, People's Republic of China*
[24] *Hunan Normal University, Changsha 410081, People's Republic of China*
[25] *Hunan University, Changsha 410082, People's Republic of China*
[26] *Indian Institute of Technology Madras, Chennai 600036, India*
[27] *Indiana University, Bloomington, Indiana 47405, USA*
[28] *INFN Laboratori Nazionali di Frascati , (A)INFN Laboratori Nazionali di Frascati, I-00044, Frascati, Italy; (B)INFN Sezione di Perugia, I-06100, Perugia, Italy; (C)University of Perugia, I-06100, Perugia, Italy*
[29] *INFN Sezione di Ferrara, (A)INFN Sezione di Ferrara, I-44122, Ferrara, Italy; (B)University of Ferrara, I-44122, Ferrara, Italy*
[30] *Inner Mongolia University, Hohhot 010021, People's Republic of China*
[31] *Institute of Modern Physics, Lanzhou 730000, People's Republic of China*
[32] *Institute of Physics and Technology, Peace Avenue 54B, Ulaanbaatar 13330, Mongolia*
[33] *Instituto de Alta Investigación, Universidad de Tarapacá, Casilla 7D, Arica 1000000, Chile*
[34] *Jilin University, Changchun 130012, People's Republic of China*
[35] *Johannes Gutenberg University of Mainz, Johann-Joachim-Becher-Weg 45, D-55099 Mainz, Germany*

[36] *Joint Institute for Nuclear Research, 141980 Dubna, Moscow region, Russia*
[37] *Justus-Liebig-Universitaet Giessen, II. Physikalisches Institut, Heinrich-Buff-Ring 16, D-35392 Giessen, Germany*
[38] *Lanzhou University, Lanzhou 730000, People's Republic of China*
[39] *Liaoning Normal University, Dalian 116029, People's Republic of China*
[40] *Liaoning University, Shenyang 110036, People's Republic of China*
[41] *Nanjing Normal University, Nanjing 210023, People's Republic of China*
[42] *Nanjing University, Nanjing 210093, People's Republic of China*
[43] *Nankai University, Tianjin 300071, People's Republic of China*
[44] *National Centre for Nuclear Research, Warsaw 02-093, Poland*
[45] *North China Electric Power University, Beijing 102206, People's Republic of China*
[46] *Peking University, Beijing 100871, People's Republic of China*
[47] *Qufu Normal University, Qufu 273165, People's Republic of China*
[48] *Renmin University of China, Beijing 100872, People's Republic of China*
[49] *Shandong Normal University, Jinan 250014, People's Republic of China*
[50] *Shandong University, Jinan 250100, People's Republic of China*
[51] *Shanghai Jiao Tong University, Shanghai 200240, People's Republic of China*
[52] *Shanxi Normal University, Linfen 041004, People's Republic of China*
[53] *Shanxi University, Taiyuan 030006, People's Republic of China*
[54] *Sichuan University, Chengdu 610064, People's Republic of China*
[55] *Soochow University, Suzhou 215006, People's Republic of China*
[56] *South China Normal University, Guangzhou 510006, People's Republic of China*
[57] *Southeast University, Nanjing 211100, People's Republic of China*
[58] *State Key Laboratory of Particle Detection and Electronics, Beijing 100049, Hefei 230026, People's Republic of China*
[59] *Sun Yat-Sen University, Guangzhou 510275, People's Republic of China*
[60] *Suranaree University of Technology, University Avenue 111, Nakhon Ratchasima 30000, Thailand*
[61] *Tsinghua University, Beijing 100084, People's Republic of China*
[62] *Turkish Accelerator Center Particle Factory Group, (A)Istinye University, 34010, Istanbul, Turkey; (B)Near East University, Nicosia, North Cyprus, 99138, Mersin 10, Turkey*
[63] *University of Bristol, (A)H H Wills Physics Laboratory; (B)Tyndall Avenue; (C)Bristol; (D)BS8 1TL*
[64] *University of Chinese Academy of Sciences, Beijing 100049, People's Republic of China*
[65] *University of Groningen, NL-9747 AA Groningen, The Netherlands*
[66] *University of Hawaii, Honolulu, Hawaii 96822, USA*
[67] *University of Jinan, Jinan 250022, People's Republic of China*
[68] *University of Manchester, Oxford Road, Manchester, M13 9PL, United Kingdom*
[69] *University of Muenster, Wilhelm-Klemm-Strasse 9, 48149 Muenster, Germany*
[70] *University of Oxford, Keble Road, Oxford OX13RH, United Kingdom*
[71] *University of Science and Technology Liaoning, Anshan 114051, People's Republic of China*
[72] *University of Science and Technology of China, Hefei 230026, People's Republic of China*
[73] *University of South China, Hengyang 421001, People's Republic of China*
[74] *University of the Punjab, Lahore-54590, Pakistan*
[75] *University of Turin and INFN, (A)University of Turin, I-10125, Turin, Italy; (B)University of Eastern Piedmont, I-15121, Alessandria, Italy; (C)INFN, I-10125, Turin, Italy*
[76] *Uppsala University, Box 516, SE-75120 Uppsala, Sweden*
[77] *Wuhan University, Wuhan 430072, People's Republic of China*

[78] *Yantai University, Yantai 264005, People's Republic of China*
[79] *Yunnan University, Kunming 650500, People's Republic of China*
[80] *Zhejiang University, Hangzhou 310027, People's Republic of China*
[81] *Zhengzhou University, Zhengzhou 450001, People's Republic of China*

[a] *Deceased*
[b] *Also at the Moscow Institute of Physics and Technology, Moscow 141700, Russia*
[c] *Also at the Novosibirsk State University, Novosibirsk, 630090, Russia*
[d] *Also at the NRC "Kurchatov Institute", PNPI, 188300, Gatchina, Russia*
[e] *Also at Goethe University Frankfurt, 60323 Frankfurt am Main, Germany*
[f] *Also at Key Laboratory for Particle Physics, Astrophysics and Cosmology, Ministry of Education; Shanghai Key Laboratory for Particle Physics and Cosmology; Institute of Nuclear and Particle Physics, Shanghai 200240, People's Republic of China*
[g] *Also at Key Laboratory of Nuclear Physics and Ion-beam Application (MOE) and Institute of Modern Physics, Fudan University, Shanghai 200443, People's Republic of China*
[h] *Also at State Key Laboratory of Nuclear Physics and Technology, Peking University, Beijing 100871, People's Republic of China*
[i] *Also at School of Physics and Electronics, Hunan University, Changsha 410082, China*
[j] *Also at Guangdong Provincial Key Laboratory of Nuclear Science, Institute of Quantum Matter, South China Normal University, Guangzhou 510006, China*
[k] *Also at MOE Frontiers Science Center for Rare Isotopes, Lanzhou University, Lanzhou 730000, People's Republic of China*
[l] *Also at Lanzhou Center for Theoretical Physics, Lanzhou University, Lanzhou 730000, People's Republic of China*
[m] *Also at the Department of Mathematical Sciences, IBA, Karachi 75270, Pakistan*
[n] *Also at Ecole Polytechnique Federale de Lausanne (EPFL), CH-1015 Lausanne, Switzerland*
[o] *Also at Helmholtz Institute Mainz, Staudinger Weg 18, D-55099 Mainz, Germany*
[p] *Also at School of Physics, Beihang University, Beijing 100191 , China*